

MVC-VPR: Mutual Learning of Viewpoint Classification and Visual Place Recognition

Qiwen Gu¹, Xufei Wang², Fenglin Zhang¹, Junqiao Zhao^{*,1,2,3}, Siyue Tao¹, Chen Ye¹, Tiantian Feng⁴, Changjun Jiang¹

¹ Department of Computer Science and Technology, School of Electronics and Information Engineering, Tongji University, Shanghai, China

² The Shanghai Research Institute for Intelligent Autonomous System, Tongji University, Shanghai, China

³ The MOE Key Lab of Embedded System and Service Computing, Tongji University, Shanghai, China

⁴ School of Surveying and Geo-Informatics, Tongji University, Shanghai, China

zhaojunqiao@tongji.edu.cn

Abstract

Visual Place Recognition (VPR) aims to robustly identify locations by leveraging image retrieval based on descriptors encoded from environmental images. However, drastic appearance changes of images captured from different viewpoints at the same location pose incoherent supervision signals for descriptor learning, which severely hinder the performance of VPR. Previous work proposes classifying images based on manually defined rules or ground truth labels for viewpoints, followed by descriptor training based on the classification results. However, not all datasets have ground truth labels of viewpoints and manually defined rules may be suboptimal, leading to degraded descriptor performance. To address these challenges, we introduce the mutual learning of viewpoint self-classification and VPR. Starting from coarse classification based on geographical coordinates, we progress to finer classification of viewpoints using simple clustering techniques. The dataset is partitioned in an unsupervised manner while simultaneously training a descriptor extractor for place recognition. Experimental results show that this approach almost perfectly partitions the dataset based on viewpoints, thus achieving mutually reinforcing effects. Our method even excels state-of-the-art (SOTA) methods that partition datasets using ground truth labels.

Introduction

Visual Place Recognition (VPR) is widely used in fields like robotics (Chen et al. 2017, 2018; Xu, Snderhauf, and Milford 2020), autonomous driving (Doan et al. 2019; Juneja, Daniušis, and Marcinkevičius 2023). The goal of a VPR system is to obtain a compact representation of a query image, compare it with a database of known geographical locations, and retrieve the most similar images to enable self-localization.

The primary challenge of VPR is to obtain invariant descriptor of a place in the presence of factors such as changing lighting conditions, seasonal variations, and changes in viewpoint. Among these factors, changes in viewpoint is especially challenging because the visual information observed from different viewpoint at the same place vary significantly. However, it is extremely difficult to learn a con-

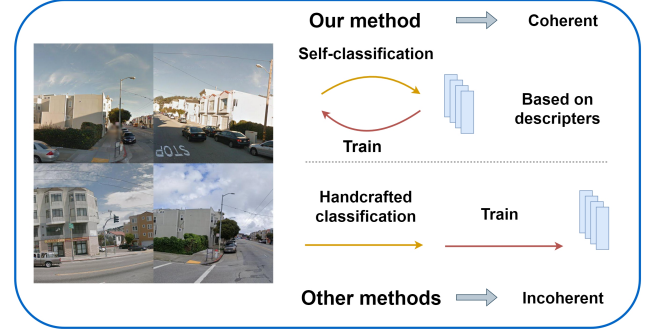


Figure 1: Compared to existing methods, our approach combines dataset self-classification with training and utilizes a vision transformer model, whereas existing methods rely on classifying the dataset before training.

sistent representation of a place with incoherent supervision signals, which leads to unstable training and performance degradation.

Existing VPR methods either utilizes contrastive learning loss (Arandjelovic et al. 2016; Wang et al. 2022; Lu et al. 2024) or the categorical cross entropy loss (Seo et al. 2018; Muller-Budack, Pustu-Iren, and Ewerth 2018; Berton, Masone, and Caputo 2022; Berton et al. 2023) to learn the place representation.

The former involves mining positive and negative samples for self-supervised contrastive learning, incurring high costs in training and making them challenging to scale to large datasets. To address the issue of viewpoint variation, (Wang et al. 2019) mines hard positive samples by evaluating their similarities to the anchor image and comparing them with the maximum similarity. While this approach reduces incoherent supervision due to viewpoint variations, it escalates mining costs and training overhead significantly.

The latter directly utilizes geographical coordinates and orientation labels to learn the representation using a classifier, significantly reducing the training cost for large datasets. Considering that different viewpoints of a place should be assigned to different classes, CosPlace (Berton, Masone, and Caputo 2022) categorizes the dataset based on

geographical coordinates and orientation labels. It classifies images from the same location according to the viewpoint label into different groups for training. Unfortunately, many datasets do not contain orientation labels, making it challenging to extend the method to other datasets.

To eliminate the need for orientation labels, EigenPlaces (Bertoni et al. 2023) proposes classifying images captured at the same location using singular value decomposition of the image position labels. This approach assumes a specific spatial distribution pattern of the images, such as those captured along roads. While effective in structured cities with regular road networks, this handcrafted rule may struggle to generalize to more varied scenarios.

To address above issues, this paper proposes a mutual learning of viewpoint self-classification. Starting from coarse classification based on geographical coordinates, we fine-tune the feature extractor using adapters to make it robust to viewpoint changes and progress to finer classification of viewpoints using simple clustering technique, as shown in Figure 1. This method categorizes the dataset in an unsupervised manner based on the descriptors obtained on-the-fly, eliminating the need for subjective handcrafted rules or ground truth labels. The experimental results demonstrate that our method enables mutual enhancement between dataset classification and training, surpassing the performance of methods that rely on ground truth labels.

The contributions can be summarized as follows:

- We propose utilizing simple K-Means Clustering for viewpoint self-classification in a VPR method with low space occupancy and high efficiency.
- We introduce a mutual learning approach, progressively classifying the dataset from coarse to fine and updating the dataset while learning, enabling mutual enforcing.
- Our method achieves state-of-the-art performance on some datasets.

Related Work

VPR has traditionally been viewed as an image retrieval problem, involving searching a database for images that match a query image within a set radius.

Modern learning-based methods significantly improve VPR accuracy by leveraging end-to-end approaches that seamlessly integrate with pre-trained backbones to create robust feature representations. NetVLAD (Arandjelovic et al. 2016) exemplifies this trend. Due to label acquisition costs, these architectures (Bertoni et al. 2021; Peng et al. 2021) utilize contrastive learning, employing triplet losses to mine positive and negative examples within the dataset for training. To address challenging sample variations, advanced strategies like AP loss (Chen et al. 2020) and Multi-Similarity loss (Wang et al. 2019) are introduced to enhance descriptor robustness.

However, these methods do not adequately address the issue of erroneous supervision arising from viewpoint variations. Conv-AP (Ali-bey, Chaib-draa, and Giguere 2022) and MixVPR (Ali-Bey, Chaib-Draa, and Giguere 2023) attempt to mitigate the impact of viewpoint changes by training on the GSV-Cities dataset (Ali-bey, Chaib-draa, and

Giguere 2022), which is divided into classes in such a way that all classes do not have distinct viewpoints but rather share the same viewpoints, aiming to reduce the effects of viewpoint changes. Other methods (Cao, Araujo, and Sim 2020; Hausler et al. 2021; Zhu et al. 2023) focus on local features and keypoint matching to enhance robustness against viewpoint variations. Yet, this often involves a two-stage process, leading to significant computational costs.

An alternative approach in VPR is to treat it as a classification problem. Methods like CosPlace (Bertoni, Masone, and Caputo 2022) and EigenPlaces (Bertoni et al. 2023) train feature extractors in a classification manner to reduce costs while maintaining high accuracy comparable to contrastive learning.

CosPlace (Bertoni, Masone, and Caputo 2022) divides the dataset into geographical cells based on coordinates and further classifies them by image orientation, enabling classification of images from the same location but different viewpoints. However, manually categorize the dataset using labels may overlook subtle spatial cues like being very similar but still being categorized into different classes, hindering comprehensive learning of varying views from a single location.

Our proposed method eliminates manual specifications by using K-Means and a training strategy that combines self-classification and VPR training. This approach achieves near-perfect viewpoint classification performance, outperforming CosPlace using true viewpoints and rivaling complex classification methods.

Method

Drastic appearance changes of images captured from different viewpoints at the same location pose incoherent supervision signals for descriptor learning. To address this issue, we propose an unsupervised viewpoint self-classification method. As shown in Figure 2, this method iteratively updates the partitioning of the dataset while training the model with the VPR classification objective. These processes alternate and mutually reinforce each other. By training the model to differentiate between different viewpoints of the same location, we aim to enhance the robustness of the model and reduce the impact of viewpoint change on descriptors.

Mutual Learning Viewpoint Self-Classification

Geo Classification. Our method initially divides the dataset into units based on geographical locations for a coarse classification. We partition images within a certain grid range based on UTM coordinates north, east, but at this stage, we do not divide them based on viewpoints. This initial coarse classification is referred to as UTM class, which can be formally expressed as:

$$x = \left\{ \left\lfloor \frac{east}{M} \right\rfloor = e_i, \left\lfloor \frac{north}{M} \right\rfloor = n_j \right\}, \quad (1)$$

where M is a hyperparameter that determines the size of the grid.

Self Classification. Before commencing training in each round, we perform fine classification within the groups of

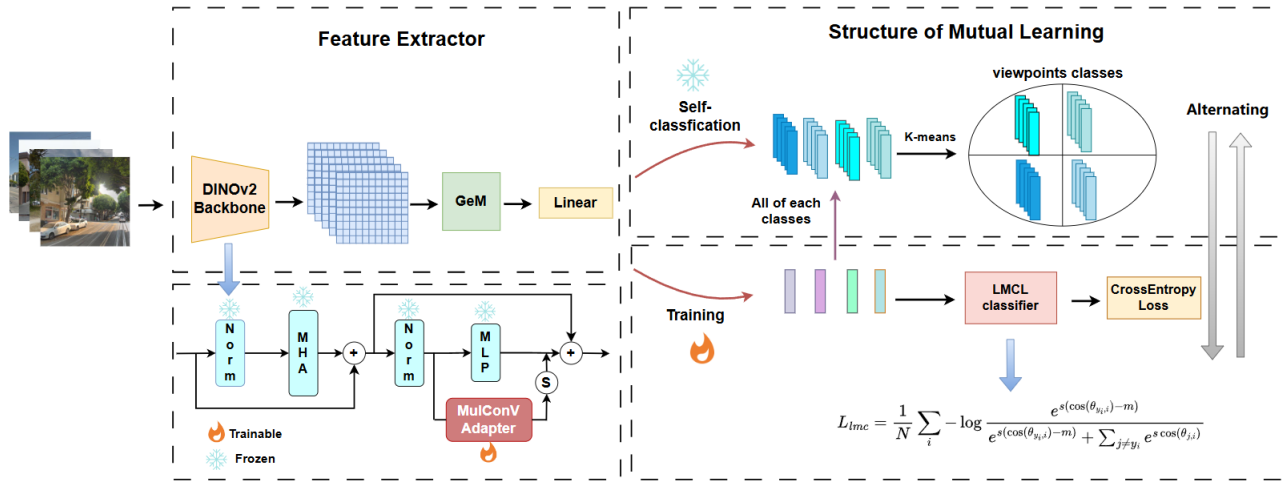


Figure 2: The overall architecture of the model. In the lower section, during the training process, all parameters except for the Adapter are frozen. The feature extractor is trained using LMCL in a classification manner. In the upper section, the self-classification process takes place where all parameters are frozen. Each time, images from the same class (same object from different viewpoints) are inputted. Features are extracted, clustered, and the results are used to update classes based on the viewpoints division. Self-classification and training proceed alternately, mutually reinforcing each other until the training is completed. It is important to note that in the self-classification depicted in the figure, all instances belong to a same class, but K-Means clustering is applied to each classes.

UTM classes. Specifically, we freeze the network model, extract features for each UTM class, and cluster all images within each UTM class based on these features. Since the ultimate goal of the VPR task is retrieval based on distances between descriptors, therefore, we employ distance-based K-Means clustering to cluster UTM classes, obtaining a viewpoint symbol C , represented as:

$$C = \{e_i, n_j, h | e_i, n_j \in x, h \in k\}, \quad (2)$$

where k is the number of clusters, which determines the granularity of viewpoint division.

Mutual Learning. The groups with viewpoint symbols obtained from fine classification are used for training. After each epoch, the current feature extractor is used to update the UTM classes within the group. It is important to note that the viewpoint labels obtained earlier might change, thereby facilitating more accurate classification through training and classification feedback loops that enhance the robustness of descriptors.

Model structure

For images captured from different viewpoints at the same location, there are often overlapping areas or shared semantic information, such as buildings from various directions at a specific site. MulConv proposed by CricaVPR (Lu et al. 2024) introduces a multi-scale convolution layer, which enables the model to capture image features across different scales. So we choose DINOv2 (Oquab et al. 2023) as the backbone and use MulConv adapter for fine-tuning, which is similar to CricaVPR (Lu et al. 2024).

Our network architecture begins with DINOv2 enhanced with the MulConv Adapter and incorporate the adapter into

a general transformer encoder. It can be expressed as

$$\begin{aligned} z'_l &= \text{MHA}(\text{LN}(z_{l-1})) + z_{l-1}, \\ z_l &= \text{MLP}(\text{LN}(z'_l)) + s \cdot \text{Adapter}(\text{LN}(z'_l)) + z'_l. \end{aligned} \quad (3)$$

The descriptor Z_l is the combination of a transformer encoder and an adapter. Initially, the input is normalized and passed through a multi-head attention layer (MHA) with residual connections to z'_l . Subsequently, z'_l is normalized and split into two branches. One branch contains the original MLP layer, while the other branch incorporates the adapter MulConv. A scaling parameter s is utilized to adjust the scale of the adapter. Finally, the output of the adapter branch is added to z'_l to derive our descriptor.

Since the images processed through DINOv2 remain in the form of patch tokens, we opt for the simple and effective GeM as our pooling method. Followed by passing through GeM pooling and projecting the features through a linear layer to the desired dimensionality, serving as the final descriptor.

We chose the Large Margin Cosine Loss (LMCL) (Wang et al. 2018) as the classification loss, same to CosPlace (Bertone, Masone, and Caputo 2022). It should be noted that the classifier is only utilized during training; during the inference phase, descriptors are directly obtained using the feature extractor for image retrieval.

Experiments

Dataset and evaluation metrics

The experimental training set utilize the SF-XL (Bertone, Masone, and Caputo 2022) dataset, while during testing, multiple commonly used VPR datasets are employed,

Dataset	Database	Query
SF-XL-train	5.6M	
SF-XL-test	2M	1000
SF-XL-val	8K	8064
Pitts250k-test	84K	8280
Pitts30k-test	10K	6818
Tokyo24/7-test	76K	315

Table 1: **Experimental dataset statistics.** The absence of a query in the SF-XL-train dataset is due to its design for a classification-based VPR task, where query is not required during training.

namely Pitts30k (Arandjelovic et al. 2016), Pitts250k (Arandjelovic et al. 2016), Tokyo24/7 (Torii et al. 2015), and SF-XL test v1. These datasets encompass significant challenges in VPR, including variations in lighting conditions, viewpoints, and time. SF-XL is a large-scale training set comprising images of the same location over several years. There are also subsets with fewer images than the original dataset. We select a subset of approximately 5.6 million images from SF-XL for training. The number of images in the datasets used for experiments is summarized in Table 1.

For evaluation, we employ the standard Recall@K metric, defined as the ratio of correctly located queries to the total number of queries. Correct localization involves searching for positive examples by matching images within a given query radius threshold based on geographical coordinates.

Implementation details

The experiment is executed on a server with three NVIDIA RTX 3090 GPUs, using PyTorch for training and testing. DINOv2’s ViT-B 14 is employed as the backbone network, with all parameters frozen except for the Adapter. Input image size is resized from 512x512 to 504x504 to meet the input requirements of ViT-B 14. The backbone network output dimensions are 14x768. GeM pooling and a fully connected layer reduce the dimensionality to 512 for the final descriptor. For dataset classification, margin M is set to 10, N is set to 5 and UTM classes are split into 8 groups, and k clusters are set to 3. The MuConv Adapter had a bottleneck ratio of 0.5, with input dimension 768 and bottleneck layer dimension 384. Three convolutional layers (1x1, 3x3, 5x5) had output dimensions 192, 96, 96 respectively, and scaling factor s is 0.2. To control training time due to the huge dataset, one-fifth of the training set is randomly selected for classification each epoch.

Testing use a 25-meter threshold for correct queries. Comparative tests against ground truth label classification are conducted to validate the mutual learning approach.

For viewpoint classification accuracy validation, when comparing the performance with ground truth methods, the number of cluster is set with K=6, matching ground truth label categories. The Hungarian algorithm (Kuhn 1955) is used for bipartite matching between clustering and ground truth results to calculate accuracy.

Comparison with other methods

We conducted a comparative analysis of our proposed method with NetVLAD, CosPlace, MixVPR, EigenPlaces, and CricaVPR on the datasets. The comparative results can be found in Table 2.

MixVPR and CricaVPR are both contrastive learning-based methods and represent the current SOTA in contrastive learning approaches. MixVPR trains on a pre-categorized dataset, benefiting from shared viewpoints that avoid erroneous supervision signals. CricaVPR utilizes a multi-scale approach, correlating features from the same location in image sequences to capture multi-scale features. While both methods generally perform well, our approach outperforms them on SF-XL and Tokyo24/7 datasets. Importantly, our method does not require sample mining, significantly reducing overhead costs.

CosPlace and EigenPlaces are classification-based methods and are also currently the SOTA. The SF-XL test set poses significant challenges due to its diverse viewpoints and lighting variations. EigenPlaces excels with an R@1 of 83.8%, yet its intricate classification methods lack clarity. In contrast, our method, employing viewpoint clustering, is straightforward, efficient, and outperforms alternatives except EigenPlaces. Compared to CosPlace’s 64.8% R@1 with direct ground truth labels, our method achieves 77.0%, marking a notable advancement. This underscores the value of phased viewpoint classification in facilitating the model’s understanding of correlations within images of identical locations.

In Tokyo24/7, our method outperforms EigenPlaces notably with an R@1 of 91.1%. This dataset features images of the same spots at various times with some viewpoint overlap, enabling our viewpoint classification to enhance location categorization, even amid substantial seasonal changes. The presence of both day and night queries in Tokyo24/7 underscores the efficacy of our approach, training while classifying viewpoints to tackle lighting variations effectively.

Concerning the Pitts250k and Pitts30k datasets with multiple yaw-angle images, our method can categorize them. However, the presence of pitch angles introduces perceptual challenges, diminishing performance. Nonetheless, on Pitts250k, our approach achieves an exceptional R@5 of 96.2%.

Notably, our method employs 512-dimensional descriptors, contrasting with superior methods using over 2048 dimensions. This trade-off, utilizing less memory for a slightly narrower performance gap, proves acceptable under resource constraints.

Viewpoint self classification analysis

One of our experimental objectives is to partition viewpoints through a simple unsupervised clustering method. In the experiment, we utilized K-Means as the clustering approach. To evaluate the accuracy of our viewpoint self-classification, we randomly selected 100 classes from each of the 8 groups in the training set, totaling approximately 100k images. For each class, we performed clustering and calculated the average accuracy using the Hungarian algorithm (Kuhn 1955) to compare the clustering results with ground truth.

Method	Desc.dim.	Train set	Pitts250k		Pitts30k		Tokyo24/7		SF-XL-testv1	
			R@1	R@5	R@1	R@5	R@1	R@5	R@1	R@5
NetVLAD	32768	Pitts250k	81.7	90.8	81.3	90.7	58.4	72.4		
MixVPR	4096	Gsv-cities	94.3	98.2	91.6	95.5	87.0	93.3	69.2	77.4
CricaVPR	4096	Gsv-cities	94.3	98.6	91.3	96.0	85.1	91.7	56.6	69.9
EigenPlaces	512	SF-XL	93.9	98.0	92.3	96.1	84.8	94.0	83.8	89.6
CosPlace	512	SF-XL	90.4	96.6	89.6	94.9	76.5	89.2	64.8	73.1
MVC-VPR(Ours)	512	SF-XL	92.1	97.7	89.6	96.2	91.1	97.1	77.0	84.6

Table 2: **Comparisons of various methods on popular datasets.** Above the middle horizontal line is the method based on contrastive learning, below is the method based on classification and our method. The reason for not testing NetVLAD on SF-XL is due to its excessively high-dimensional descriptors, which exceed memory limitations. It can be observed that our method outperforms others on certain datasets.

Method / Diff.	Augment	Accuracy
DINOv2	N	0.88
DINOv2	Y	0.78
Difference		0.10
CricaVPR	N	0.92
CricaVPR	Y	0.86
Difference		0.06
MVC-VPR(Ours)	N	0.98
MVC-VPR(Ours)	Y	0.96
Difference		0.02

Table 3: **Accuracy of viewpoint classification.** The accuracy in the table is obtained by extracting descriptors with the corresponding method, clustering them using K-Means on SF-XL. The difference reflects the robustness of descriptors to classification under different viewpoints when faced with data augmentation. Data augmentation techniques included adjustments to brightness, random cropping, and others.

To demonstrate that our mutual learning approach aids in better viewpoint classification, we compared the performance of our method with the untrained DINOv2 model and the CricaVPR model based on DINOv2. We also made the dataset more challenging through data augmentation. The results are presented in Table 3.

Clearly, our method achieved nearly perfect viewpoint classification with an accuracy of 0.98 on SF-XL. Furthermore, the difference in performance indicates that DINOv2 exhibits weaker robustness to augmented images before training, while CricaVPR shows some improvement after training. Even after data augmentation, our method only deviated by 0.02 in accuracy, further illustrating how the training strategy of mutual learning helps the model learn more robust features under different viewpoints.

Subsequently, to validate the transferability of viewpoint classification, we conduct testing on Pitts250k and performed qualitative analysis. Because Pitts250k contains

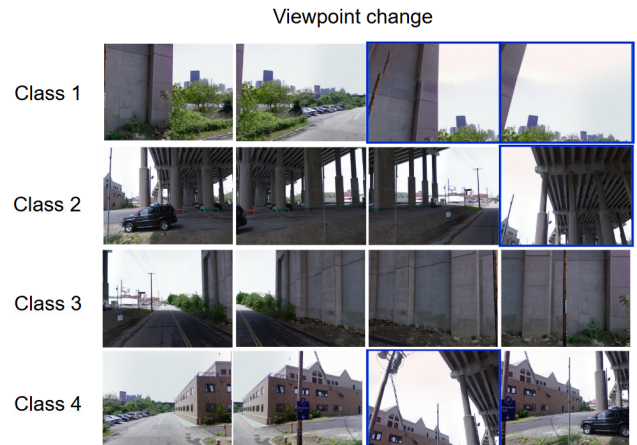


Figure 3: **Qualitative results of viewpoint classification.** The images in the table are sourced from Pitts250k. We set the number of clusters to 4 to categorize viewpoints into 4 classes. The blue boxes indicate images influenced by pitch, yet our method still correctly assigns them to the appropriate class.

ground truth labels for yaw and pitch, yet unlike the SF-XL dataset where multiple images exist for the same viewpoint, each viewpoint in Pitts250k is represented by only a single image, we are unable to perform quantitative analysis and calculate accuracy. Given our method's focus on viewpoint, we primarily considered yaw. It is worth noting that the presence of pitch introduces some interference in viewpoint classification, but our method still performs well in classification, as shown in Figure 3. Since Pitts250k lacks strict angle labels like SF-XL, the angle variations between images may be inconsistent. However, our method still successfully groups images with similar yaw labels into the same class.

Ablation

Ground Truth. To demonstrate the effectiveness of our proposed mutual learning method, we designed experiments to compare the co-learning approach with the ground truth method. CosPlace was initially trained on CNN. We re-

Method / Diff.	Backbone	Tokyo24/7		SF-XL-testv1	
		R@1	R@5	R@1	R@5
CosPlace	ResNet50	76.5	89.2	64.8	73.1
MVC-VPR(Ours)	ResNet50	82.9	90.2	74.5	83.3
Difference		6.4	1.0	9.7	10.2
CosPlace	DINOv2	90.2	95.5	76.8	86.3
MVC-VPR(Ours)	DINOv2	91.1	97.1	77.0	84.6
Difference		0.9	1.6	0.2	-1.7

Table 4: **The performance comparison between cluster mutual learning and ground truth learning.** The difference represents the variance between our method and CosPlace, which classifies based on ground truth labels.

Backbone	K	Tokyo24/7		SF-XL-testv1	
		R@1	R@5	R@1	R@5
ResNet50	1	54.3	71.4	30.3	40.4
ResNet50	3	81.0	89.8	73.9	81.4
ResNet50	6	82.9	90.2	74.5	83.3
DINOv2	1	80.6	91.4	61.1	71.1
DINOv2	3	91.1	97.1	77.0	84.6
DINOv2	6	86.0	94.0	70.9	79.6

Table 5: **Different Cluster Numbers.** $K = 1$ can be considered as not classifying the dataset, while $K = 6$ aims to match the number of cluster labels with the ground truth clustering labels. .

trained it using DINOv2 for a more intuitive comparison with our method. As indicated in Table 4, we conducted tests on the challenging Tokyo24/7 and SF-XL testv1 datasets, revealing that our method outperforms CosPlace in most cases.

For methods utilizing ResNet as the backbone, we observed significant improvements in R@1 on both datasets, particularly a 10.2% increase in R@5 on SF-XL. This enhancement can be attributed to ResNet’s insufficient generalization capabilities. Unlike pre-classifying datasets for training, our method trains while simultaneously clustering the dataset. The categories of images under different viewpoints are not fixed but adjust as descriptor performance improves, thereby enhancing model generalization. This reinforcement of model generalization leads to improved viewpoint classification, achieving mutual enhancement effects.

Regarding DINOv2, its performance surpasses that based on ResNet, albeit with marginal improvements. In fact, there were slight declines in R@5 on SF-XL. This is because DINOv2 already possesses excellent feature extraction capabilities and strong generalization, enabling it to initially partition the training set effectively. As a result, its performance is naturally superior from the start, with limited room for further improvement.

Cluster Number. The cluster number K is a hyperparameter in the experiment that determines how many classes viewpoints are divided into. The number of categories is

Method	K-Means	Hierarchical	Spectral
DINOv2	0.88	0.87	0.82
MVC-VPR(Our)	0.98	0.98	0.98

Table 6: **Different Clustering Methods.** Specifying the number of clusters to match the number of ground truth categories, and use the Hungarian algorithm to calculate accuracy across various clustering methods.

Backbone	Params.	Flops.	SF-XL-testv1	
			R@1	R@5
VGG16	15.0m	77.5b	61.5	70.8
ResNet50	24.6m	21.3b	73.9	81.4
DINOv2	100.9m	122.8b	77.0	84.6

Table 7: **Comparisons of various backbone.** Train under different backbones when $K=3$. For VGG16, only the parameters of the last layer are trained. For ResNet50, only the parameters beyond the third layer are trained. For DINOv2, only the adapter module is trained.

related to the granularity of the dataset partitioning. When there are fewer categories, the images within each category are more compact and exhibit greater similarity. Conversely, with a larger number of categories, viewpoints are divided more finely, resulting in greater diversity among them. In the experiment, we tested $K = 1, 3, 6$. The experimental results are shown in Table 5.

It can be observed that the performance of classification is better than not classifying the data, indicating that classifying viewpoints is effective. For DINOv2, the performance is optimal when $K = 3$, surpassing the model with the same number of classes as the ground truth. On the other hand, for ResNet50, a slight edge is still noticeable when $K = 6$, although the overall performance difference is minimal. This suggests that the choice of cluster number is not only relevant to the dataset but also to the model’s backbone. Determining the appropriate K based on the dataset and the model used remains an unresolved issue.

Cluster Method. Due to the fixed number of categories in the ground truth labels for ease of accuracy validation, we employed specific clustering methods that directly specify the number of clusters. We tested the accuracy of viewpoint clustering using K-Means, hierarchical clustering, and spectral clustering, with the results shown in Table 6.

Among these methods, K-Means performed best initially on the pre-trained DINOv2 model, while after training, the accuracies of all three methods improved and converged. Considering simplicity and effectiveness, K-Means emerged as the optimal choice.

BackBone. In Table 7, we conducted an ablation study on different backbones, comparing their parameter counts and computational loads. Although DINOv2 performs exceptionally well, it has the highest computational load and parameter count, four times that of ResNet50, with training times nearly three times longer. While VGG16’s overall

training time is similar to ResNet50, its performance is inferior to the latter. In general, despite some loss in performance, ResNet50 emerges as a favorable choice when GPU resources are limited and there are constraints on training time.

Conclusion and Future work

In this work, we propose a self-classification approach from a mutual learning viewpoint for VPR, addressing a series of issues caused by manual dataset classification in previous works. Starting from the viewpoints, we provide a solution to the problem of perceptual confusion in VPR caused by different viewpoints from the same location. Our method involves unsupervised self-classification of viewpoints, with classification and training occurring in a collaborative manner, ultimately achieving more accurate classification and robust descriptor learning through mutual reinforcement.

One limitation of our approach is that the value for the number of clusters, denoted as K , is fixed. On one hand, the compactness of viewpoints may not be entirely consistent, and on the other hand, as classification and descriptors learn from each other, the number of categories should be dynamically adjusted. Our ablation experiments also demonstrate the impact of the cluster number K on the results. Future work will continue to explore how to make K dynamically adjustable to adapt to different datasets while enhancing the connection between classification and training.

References

Ali-bey, A.; Chaib-draa, B.; and Giguere, P. 2022. Gsv-cities: Toward appropriate supervised visual place recognition. *Neurocomputing*, 513: 194–203.

Ali-Bey, A.; Chaib-Draa, B.; and Giguere, P. 2023. Mixvpr: Feature mixing for visual place recognition. In *Proceedings of the IEEE/CVF winter conference on applications of computer vision*, 2998–3007.

Arandjelovic, R.; Gronat, P.; Torii, A.; Pajdla, T.; and Sivic, J. 2016. NetVLAD: CNN architecture for weakly supervised place recognition. In *Proceedings of the IEEE conference on computer vision and pattern recognition*, 5297–5307.

Bertone, G.; Masone, C.; and Caputo, B. 2022. Rethinking visual geo-localization for large-scale applications. In *Proceedings of the IEEE/CVF Conference on Computer Vision and Pattern Recognition*, 4878–4888.

Bertone, G.; Trivigno, G.; Caputo, B.; and Masone, C. 2023. Eigenplaces: Training viewpoint robust models for visual place recognition. In *Proceedings of the IEEE/CVF International Conference on Computer Vision*, 11080–11090.

Bertone, G. M.; Paolicelli, V.; Masone, C.; and Caputo, B. 2021. Adaptive-attentive geolocalization from few queries: A hybrid approach. In *Proceedings of the IEEE/CVF Winter Conference on Applications of Computer Vision*, 2918–2927.

Cao, B.; Araujo, A.; and Sim, J. 2020. Unifying deep local and global features for image search. In *Computer Vision–ECCV 2020: 16th European Conference, Glasgow, UK, August 23–28, 2020, Proceedings, Part XX 16*, 726–743. Springer.

Chen, K.; Lin, W.; Li, J.; See, J.; Wang, J.; and Zou, J. 2020. AP-loss for accurate one-stage object detection. *IEEE Transactions on Pattern Analysis and Machine Intelligence*, 43(11): 3782–3798.

Chen, Z.; Jacobson, A.; Sünderhauf, N.; Upcroft, B.; Liu, L.; Shen, C.; Reid, I.; and Milford, M. 2017. Deep learning features at scale for visual place recognition. In *2017 IEEE international conference on robotics and automation (ICRA)*, 3223–3230. IEEE.

Chen, Z.; Liu, L.; Sa, I.; Ge, Z.; and Chli, M. 2018. Learning context flexible attention model for long-term visual place recognition. *IEEE Robotics and Automation Letters*, 3(4): 4015–4022.

Doan, A.-D.; Latif, Y.; Chin, T.-J.; Liu, Y.; Do, T.-T.; and Reid, I. 2019. Scalable place recognition under appearance change for autonomous driving. In *Proceedings of the IEEE/CVF International Conference on Computer Vision*, 9319–9328.

Hausler, S.; Garg, S.; Xu, M.; Milford, M.; and Fischer, T. 2021. Patch-netvlad: Multi-scale fusion of locally-global descriptors for place recognition. In *Proceedings of the IEEE/CVF conference on computer vision and pattern recognition*, 14141–14152.

Juneja, S.; Daniušis, P.; and Marcinkevičius, V. 2023. Visual place recognition pre-training for end-to-end trained autonomous driving agent. *IEEE access*, 11: 128421–128428.

Kuhn, H. W. 1955. The Hungarian method for the assignment problem. *Naval research logistics quarterly*, 2(1-2): 83–97.

Lu, F.; Lan, X.; Zhang, L.; Jiang, D.; Wang, Y.; and Yuan, C. 2024. CricaVPR: Cross-image Correlation-aware Representation Learning for Visual Place Recognition. In *Proceedings of the IEEE/CVF Conference on Computer Vision and Pattern Recognition*, 16772–16782.

Muller-Budack, E.; Pustu-Iren, K.; and Ewerth, R. 2018. Geolocation estimation of photos using a hierarchical model and scene classification. In *Proceedings of the European conference on computer vision (ECCV)*, 563–579.

Quab, M.; Darzet, T.; Moutakanni, T.; Vo, H.; Szafraniec, M.; Khalidov, V.; Fernandez, P.; Haziza, D.; Massa, F.; El-Nouby, A.; et al. 2023. Dinov2: Learning robust visual features without supervision. *arXiv preprint arXiv:2304.07193*.

Peng, G.; Yue, Y.; Zhang, J.; Wu, Z.; Tang, X.; and Wang, D. 2021. Semantic reinforced attention learning for visual place recognition. In *2021 IEEE International Conference on Robotics and Automation (ICRA)*, 13415–13422. IEEE.

Seo, P. H.; Weyand, T.; Sim, J.; and Han, B. 2018. Cplanet: Enhancing image geolocalization by combinatorial partitioning of maps. In *Proceedings of the European Conference on Computer Vision (ECCV)*, 536–551.

Torii, A.; Arandjelovic, R.; Sivic, J.; Okutomi, M.; and Pajdla, T. 2015. 24/7 place recognition by view synthesis. In *Proceedings of the IEEE conference on computer vision and pattern recognition*, 1808–1817.

Wang, H.; Wang, Y.; Zhou, Z.; Ji, X.; Gong, D.; Zhou, J.; Li, Z.; and Liu, W. 2018. Cosface: Large margin cosine loss for deep face recognition. In *Proceedings of the IEEE conference on computer vision and pattern recognition*, 5265–5274.

Wang, R.; Shen, Y.; Zuo, W.; Zhou, S.; and Zheng, N. 2022. Transvpr: Transformer-based place recognition with multi-level attention aggregation. In *Proceedings of the IEEE/CVF Conference on Computer Vision and Pattern Recognition*, 13648–13657.

Wang, X.; Han, X.; Huang, W.; Dong, D.; and Scott, M. R. 2019. Multi-similarity loss with general pair weighting for deep metric learning. In *Proceedings of the IEEE/CVF conference on computer vision and pattern recognition*, 5022–5030.

Xu, M.; Snderhauf, N.; and Milford, M. 2020. Probabilistic visual place recognition for hierarchical localization. *IEEE Robotics and Automation Letters*, 6(2): 311–318.

Zhu, S.; Yang, L.; Chen, C.; Shah, M.; Shen, X.; and Wang, H. 2023. R2former: Unified retrieval and reranking transformer for place recognition. In *Proceedings of the IEEE/CVF Conference on Computer Vision and Pattern Recognition*, 19370–19380.